

Ultra-Long-Span U-band Transmission Enabled by Incoherently Pumped Raman Amplification

Natsupa Taengnoi, Kyle R. H. Bottrill, Yang Hong, Lajos Hanzo, and Periklis Petropoulos

Abstract—We demonstrate U-band Raman amplification in non-zero dispersion shifted fibre, exploiting the amplified spontaneous emission of an erbium-doped fibre amplifier as a broad-bandwidth, incoherent pump for low-noise amplification. By doing so, we achieve a high overall gain of ~ 22 dB over a ~ 2.6 -THz 3-dB bandwidth and obtain an average noise figure of ~ 4 dB in a 40km-long, discrete amplifier configuration, in both forward pumped and backward pumped scenarios. The performance of the U-band Raman amplification is also studied through transmission of a coherent signal over a 285-km point-to-point link. This work represents, at the time of writing, the longest-reach single-span U-band transmission demonstrated.

Index Terms— broadband communication, nonlinear optics, optical amplifiers, optical fibre amplifiers, optical fibre communication, Raman scattering.

I. INTRODUCTION

Over the past decade, there have been increasing efforts to exploit a wider proportion of the transmission window of standard single-mode fibre (SMF) for high-capacity data transmission. The conventional band or C-band, centred around the wavelength of 1550 nm, has been commonly exploited, thanks to its coincidence with both the lowest-loss region of SMFs and the gain region of the erbium-doped fibre amplifier (EDFA) which offers low-noise amplification. In commercial systems, wavelength-division multiplexing (WDM) has been extensively leveraged to efficiently utilise the ~ 4.4 THz of bandwidth available in the C-band. Beyond this, the short and long bands, namely S- and L-bands (see Fig. 1), have received much attention [1], since doped-fibre amplifiers can be designed to offer gain at these wavelengths. Besides these, the even shorter wavelength original and extended bands (O- and E-bands, respectively), have also been used for data transmission, albeit generally in short reach (often single-span, unamplified) systems.

Although there are a number of transmission and amplifier

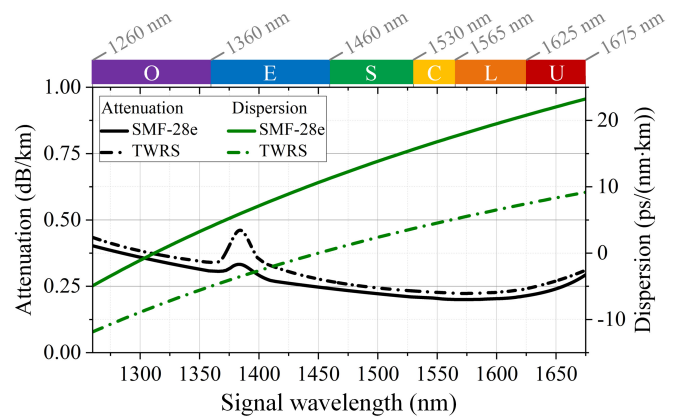


Fig. 1. Wavelength dependence of parameters from O- to U-band of SMF-28e and TWRS in terms of attenuation and dispersion.

demonstrations ranging from the O- to the L- band [2,3], the ultra-long band (U-band, 1625-1675 nm, equivalent to a ~ 5.5 THz bandwidth), is often overlooked for communication. Fig. 1 provides plots of the attenuation and chromatic dispersion of two fibres, the well-known Corning SMF-28e fibre and OFS TrueWave-RS (TWRS), the fibre used in this work on account of its high Raman gain coefficient [4]. The figure highlights that this entire region can be considered for transmission in silica fibres, even though dispersion management requirements will vary considerably across the spectrum. One of the main challenges in utilising the U-band is the availability of effective, low-noise amplification. With regards to doped-fibre amplifiers, alternative dopants to erbium may offer gain in the U-band. One such candidate dopant is bismuth, which has been reported to be able to offer gain in bands spanning a wavelength range of 1150-1500 nm and 1600-1800 nm [5]. Unfortunately, bismuth suffers from a low power conversion efficiency in this wavelength region [6]. Furthermore, it should also be noted that some important behavioural characteristics of bismuth are still not well

Manuscript received month date, year; revised month date, year; accepted month date, year. Date of publication month date, year; date of current version month date, year. This work was supported by the UK's EPSRC under the Airguide Photonics, COALESCE, and PHOS grants (EP/P030181/1, EP/P003990/1, EP/S002871/1). (Corresponding author: Natsupa Taengnoi.)

For the purpose of open access, the author has applied a creative commons attribution (CC BY) licence to any author accepted manuscript version arising. Open access data for this work is available at doi: xxxx.

Natsupa Taengnoi is with Optoelectronics Research Centre, University of Southampton, Southampton SO17 1BJ, U.K., on leave from the Department of

Electrical Engineering, Kasetsart University, Bangkok 10900, Thailand. (e-mail: n.taengnoi@soton.ac.uk, fengnut@ku.ac.th)

Kyle R. H. Bottrill and Periklis Petropoulos are with Optoelectronics Research Centre, University of Southampton, Southampton SO17 1BJ, U.K. (e-mail: k.bottrill@soton.ac.uk and pp@orc.soton.ac.uk).

Yang Hong was with Optoelectronics Research Centre, University of Southampton, Southampton SO17 1BJ, U.K.. He is currently with Nokia Bell Labs, Paris-Saclay, Nozay, 91620, France (e-mail: yang.hong@nokia.com)

Lajos Hanzo is with School of Electronics and Computer Science, University of Southampton, Southampton SO17 1BJ, U.K. (e-mail: lh@ecs.soton.ac.uk).

understood [3,7]. Several numerical studies suggested that praseodymium dopants can provide gain in the U-band region [8,9], but its practicality is generally compromised by the need to use a fluoride-glass host and high pump power [3]. Thulium-doped fibres have been used extensively to obtain gain at wavelengths beyond 1600 nm. However, their use in lasers and amplifiers operating below ~ 1750 nm is challenging, since it generally requires high-power pumping and some means to suppress the longer wavelength amplified spontaneous emission (ASE) [10]. Nevertheless, a thulium-doped fibre amplifier was demonstrated to offer a 12-24 dB gain over the 1628-1655 nm range, but this was achieved using a double-pass configuration (which is known to degrade the noise figure (NF) [11]) and required a rather high pump power of 36.9 dBm [10]. On the other hand, semiconductor optical amplifiers (SOA) can be designed to deliver gain over a wide variety of wavelengths and, in some cases, with a very wide bandwidth [12]. Unfortunately, when compared with rare-earth doped fibre amplifiers, amplification in SOAs may suffer from a poorer NF due to higher coupling losses, a higher polarisation sensitivity, stronger inter-channel crosstalk due to gain saturation [3], and higher nonlinear degradation [13].

In this context, Raman amplification (RA) is a viable option for the U-band, thanks to its versatile operating wavelength. The pump wavelength required for obtaining gain at the centre of the U-band (1650 nm) is conveniently located at ~ 1530 nm, where an abundance of sources and high-power amplifiers is available, and where the propagation of the pump wave in silica fibres occurs at minimum loss in SMF. The availability of high-power pumps is especially useful for obtaining high gain, given the decreased Raman gain efficiency in the U-band compared to shorter wavelength regions [3]. Moreover, the U-band has a lower Rayleigh scattering coefficient and higher dispersion than shorter wavelength bands and therefore, U-band RA is likely to experience reduced noise due to double Rayleigh scattering as well as reduced degradation from Kerr nonlinearity. An early demonstration of a U-band RA with counter-pumping configuration was presented in [14] providing a peak gain of 31.6 dB, gain bandwidth ≥ 50 nm, and NF below 6.5 dB.

The use of incoherent pumping of RAs has been shown to both reduce the relative intensity noise (RIN) penalty [15] and flatten the gain profile [16]. In the U-band, this can be implemented conveniently using the ASE of an EDFA as the pump. This will be demonstrated in this work, using a 40-km length of non-zero dispersion shifted fibre (NZDSF) as the gain medium. Both forward (FW) and backward (BW) pumping configurations are considered, achieving a net gain of 21.7 dB over a 23.5-nm (1646.7-1669.9 nm) bandwidth, equivalent to ~ 2.6 THz, and a low NF of ~ 4 dB. Motivated by studies showing that distributed RA implementations are particularly suitable for ultra-long-span transmission [17], we subsequently use our findings to demonstrate single-span transmission over 285 km of NZDSF. This demonstration is, to the best of our knowledge, the longest-reach single-span U-band transmission. We present a characterisation of the link and validate its performance through the transmission of an 18.4 Gb/s dual-polarisation binary phase-shift keying (DP-BPSK) signal. This

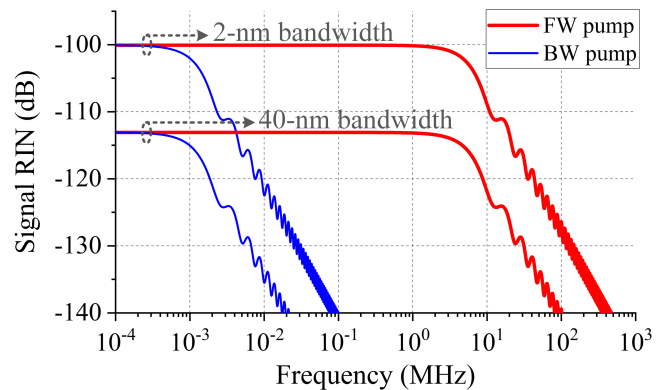


Fig. 2. RIN spectra of the signal that were transferred from the pumps with two different bandwidths, 2 nm and 40 nm, when pumping in FW (red) and BW (blue) directions. The optical field shape of the pumps was given to be a rectangle. The values of Raman parameters used for the numerical plots are as follows: signal wavelength = 1650 nm, pump wavelength = 1538.3 nm, pump attenuation = 0.21 dB/km, pump power = 940 mW, fibre length = 40 km, dispersion = 19.1 ps/(nm·km), Raman gain efficiency = $0.296 \text{ (W} \cdot \text{km)}^{-1}$.

paper extends the work presented at the 48th European Conference on Optical Communication (ECOC) conference [18].

II. U-BAND DISCRETE RAMAN AMPLIFICATION – DESIGN AND EXPERIMENTAL SETUP

In order to obtain Raman gain in the U-band, pumps located in the C-band are needed. Although high-power laser diodes can be used for this purpose [19], the use of amplified spontaneous emission (ASE) produced from EDFAs is arguably a more attractive option, since its wideband nature contributes to the mitigation of RIN transfer from pump to signal. To illustrate this benefit, estimates of signal RIN due to pump RIN transfer after RA are plotted in Fig. 2, using the formulae derived in [20], for FW and BW pump configurations. Two pump scenarios are shown: pumping with a 2-nm bandwidth source and pumping with a 40-nm bandwidth source. To calculate the initial pump RIN, the pump spectra are assumed to be rectangular [21]. As shown in Fig. 2, signal RIN degradation is noticeably reduced when a broader pump bandwidth is adopted. This is because, even though the total (integrated) RIN of these two sources is the same, the broader bandwidth pump will contain a greater proportion of its RIN at higher frequencies than a narrower bandwidth pump. These higher frequencies will be more rapidly averaged out than lower-frequency components (either through dispersion and/or counter-propagation). RIN transfer in Raman amplifiers is reduced through walk-off between the signal and pump(s). The extent of walk-off is largely determined by dispersion in the FW case but is instead determined by counter-propagation of the pump and signal in the BW case and hence, RIN transfer is much more rapidly suppressed in the BW case than in the FW case.

Figs. 3(a) and 3(b) show the experimental setups of the U-band discrete RA with incoherent pumping from C-band EDFAs in the FW and BW directions, respectively. To facilitate a comparison with the bidirectionally pumped transmission link

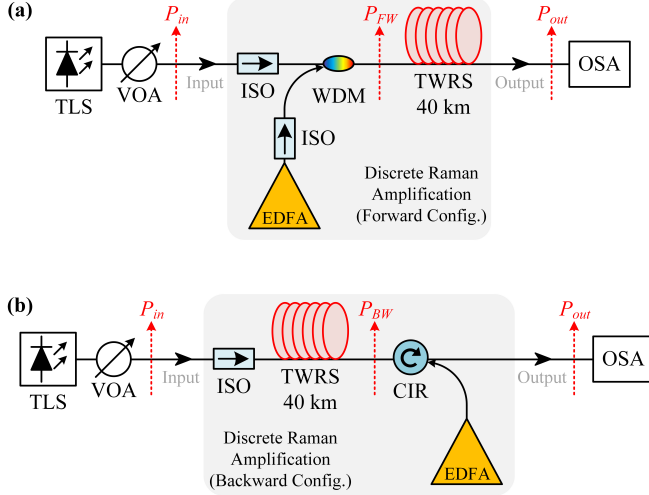


Fig. 3. Experimental setups of 40-km discrete Raman amplification: (a) forward pumping scheme and (b) backward pumping scheme. The indicators (dashed arrows) P_{in} , P_{out} , P_{FW} , and P_{BW} are the measurement points for input power, output power, FW-pump power, and BW-pump power, respectively.

that will be demonstrated in the following section, the pump sources employed in the FW and BW configurations were the same as those used in the bidirectional pumping case. The gain medium was a 40-km spool of TWRS. TWRS was reported to have higher Raman gain efficiency than SMF by a factor of >1.6 (measured in the C-band) [4]. The total loss of the fibre spool was measured to be 9.1 dB at 1550 nm and 10.8 dB at 1650 nm, with an effective length of ~ 20 km. (Note that even though this fibre length was not ideal for the application, it was chosen since it was the shortest length available in the lab.) For the FW pumping case, as shown in Fig. 3(a), the C-band ASE pump was propagated through an isolator (ISO) to prevent any back scattering. Then it was coupled into the gain fibre through a WDM coupler. The FW-pump power (P_{FW}) was determined immediately after the WDM coupler (see the measurement point indicated in the setup). As for the BW pump shown in Fig. 3(b), the ASE pump was combined into the fibre using a circulator (CIR) and the corresponding pump power (BW-pump power, P_{BW}) was determined immediately after the circulator. After passing through the gain fibre, the amplified signal was extracted using the third port of the circulator.

To characterise the RA, a continuous wave (CW) tuneable laser source (TLS) was added into the testbed with a tuneability wavelength range of 1449-1651 nm. This range did not allow us to perform characterisation across the full bandwidth of the Raman gain, which extended beyond 1660 nm. A variable optical attenuator (VOA) was placed after the TLS to adjust the input power (P_{in}) of the RA section. Then at the RA output, the output power (P_{out}) was determined and the amplified signal was analysed using an optical spectrum analyser (OSA).

III. U-BAND DISCRETE RAMAN AMPLIFICATION – EXPERIMENTAL RESULTS AND DISCUSSION

Fig. 4 shows wideband spectra covering the pump and gain

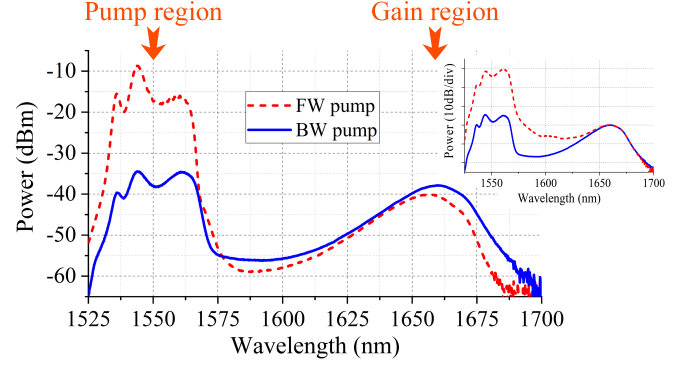


Fig. 4. Power spectra captured by OSA for the U-band discrete RAs from FW and BW pumping schemes. The OSA resolution was 0.01 nm. The inset spectra were measured when using the same EDFA for the FW and BW cases.

regions for the FW and BW pumping discrete RAs with an equal pump power of 29.73 dBm (940 mW). The BW case has a higher Raman ASE, which is mainly due to the BW pump offering the highest gain near the output of the amplifier (where the measurement was taken). The resultant Raman ASE for FW pumping has a peak around 1657 nm and a 3-dB bandwidth of ~ 23 nm (2.5 THz). Whilst the gain region from the BW pump has a peak around 1660 nm and a ~ 24 -nm bandwidth (2.6 THz). These small differences are largely due to the differing pump spectra, which arise from the use of two EDFAs of different construction to supply each of the two pump sources in this characterisation, although the additional loss of the fibre approaching 1700 nm also contribute (to a very small extent) to the deviation. To illustrate this, the inset of Fig. 4 shows a one-off measurement performed by launching the exact same pump spectra into both the forward and backward pumping directions and, in this case, the gain spectra can be seen to be almost identical. Note also that the difference in spectral power around the pump region of the FW and BW pumps is simply because the BW pump can only be observed from Rayleigh scattering into the forward direction, whereas the FW pump naturally propagates in the forward direction.

Fig. 5(a) provides a characterisation of the optical gain and NF against signal wavelength at an input power of -20 dBm. The gain profiles show that it is possible to provide a gain >20.4 dB for the FW case and >21.5 dB for the BW case beyond 1651 nm, our longest testable wavelength. The benefit of utilising a broadband ASE pump for RA is also exemplified by the very flat shape (<0.5 dB variation) of the resultant NFs across the wavelengths. The average NFs are approximately 4 dB and 4.9 dB for FW and BW pumping, respectively. The FW pump RA has a lower NF, since the peak gain occurs at the beginning of the fibre, and can therefore maintain better the signal optical signal-to-noise ratio (OSNR) during signal propagation [22].

The effect of input signal power on the RA performance is investigated next, see Fig. 5(b). Increasing the input power beyond -20 dBm noticeably affects the NF of the FW pumping case more substantially than in the BW case. This is due to a much stronger RIN transfer from the pump to the signal in the

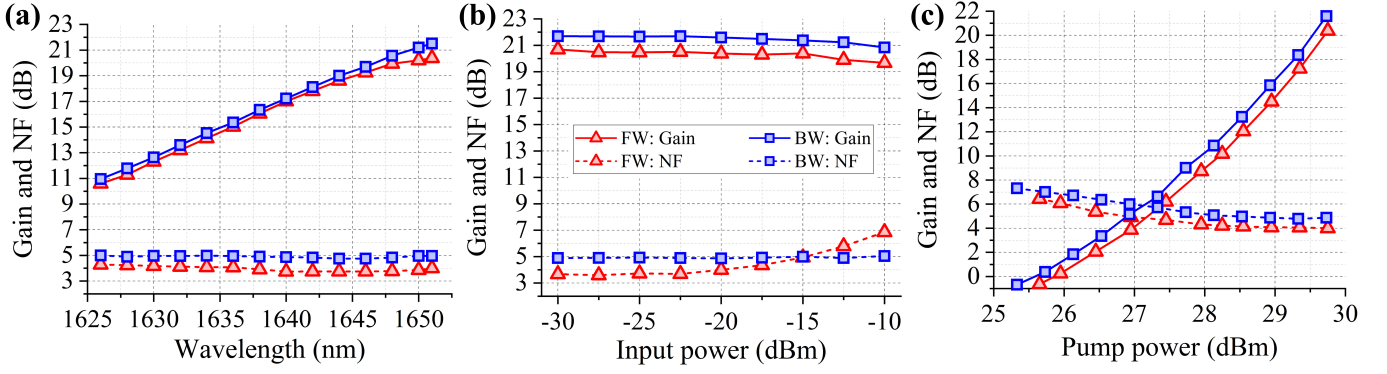


Fig. 5. Gain and NF profiles for FW and BW pumping cases of the discrete RAs measured at (a) various signal wavelengths with $P_{in} = -20$ dBm and $P_{FW} = P_{BW} = 29.73$ dBm, (b) various input powers with $\lambda_{sig} = 1651$ nm and $P_{FW} = P_{BW} = 29.73$ dBm, and (c) various pump powers with signal wavelength = 1651 nm and $P_{in} = -20$ dBm. Note that the OSA resolution used to measure optical NF was 0.1 nm.

FW pumping case. Although this was buried beneath the ASE for lower input signal powers, it became observable at higher input signal powers. Furthermore, the onset of pump depletion (leading to gain saturation) can also be observed in the gain profiles for input powers higher than -17.5 dBm. Shortening the gain fibre and increasing the pump power to maintain the same gain is one possible approach to delaying the onset of depletion. Finally, Fig. 5(c) shows that increasing the pump power results in higher gain and lower NF, with the FW case requiring ~ 0.25 dB higher pump power than the BW case to attain the same gain.

IV. U-BAND LINK UTILISING DISTRIBUTED RAMAN AMPLIFICATION – EXPERIMENTAL SETUP

In this section, we make use of RA in a distributed manner to validate its performance for U-band transmission, targeting ultra-long-haul single span transmission in 285 km of NZDSF. The experimental setup of the distributed RA is presented in Fig. 6(a). The distributed RA was pumped at each end of the gain fibre by the very same configurations of the FW and BW pumping schemes as presented in the previous sections. The gain/transmission fibre used in this demonstration was composed from a combination of lengths available in the lab at the time of the experiment, namely 160-km of TWRS and

125-km of Corning LEAF. The total loss of the 285-km fibre measured at 1550 nm and 1650 nm was 50.6 dB and 59.8 dB, respectively. A coherent transmitter and receiver were added to this configuration (Fig. 6(b)), to transmit a dual polarisation BPSK signal. This format was chosen, since it was found that the C-band dual-drive Mach-Zehnder modulator (DD-MZM) employed offered much lower loss in the U-band than the C-band IQ-modulators that were available. Firstly, a 9.2-Gbit/s BPSK signal was generated using a DD-MZM. The modulated signal was then split by a 50:50 coupler. A delay of ~ 400 symbols was applied to one of the two copies of the signal using a delay-line (DL), before they were multiplexed using a polarisation beam splitter (PBS) onto orthogonal polarisations. Consequently, a 9.2-GBd DP-BPSK signal was obtained at the output of the transmitter and launched with a power of $P_{tx} = 9.3$ dBm into the link. At the link output, a VOA was used to adjust the received optical power (P_{rx}), followed by a 99:1 coupler that facilitated power spectral measurements on an OSA. An optical bandpass filter (OBPF) with a bandwidth of ~ 1.6 nm (at 10-dB bandwidth) was used to eliminate the out-of-band ASE from the signal, following which the signal was passed to an intradyne coherent receiver to analyse the signal quality.

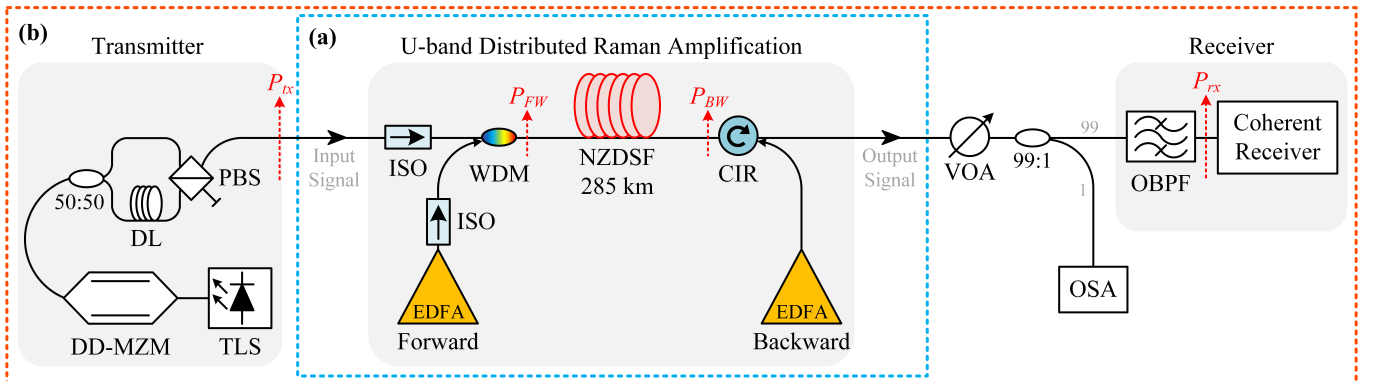


Fig. 6. Experimental setup for (a) U-band distributed Raman amplified transmission link using bidirectional ASE pumps and (b) amplified U-band point-to-point link. The indicators (dashed arrows) P_{tx} , P_{rx} , P_{FW} , and P_{BW} are the measurement points for launched power, received optical power, FW pump power, and BW pump power, respectively.

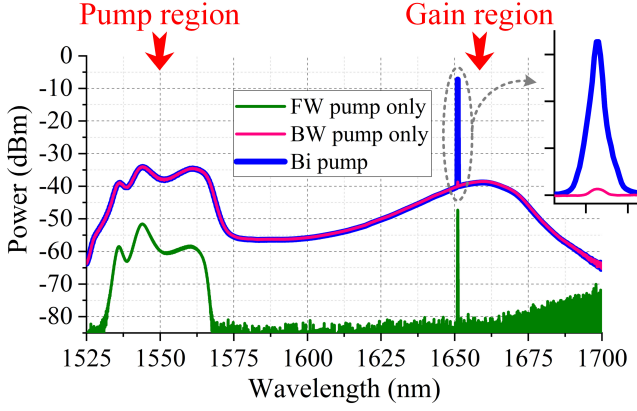


Fig. 7. Power spectra captured by OSA for the U-band distributed RA from FW pump only, BW pump only, and bidirectional (Bi) pump. Inset is the zoom-in spectra. The OSA resolution was 0.01 nm. Note that the OSA sensitivity was low around 1700 nm, which appeared as the increasing noise in the FW case's spectra.

V. U-BAND LINK UTILISING DISTRIBUTED RAMAN AMPLIFICATION – EXPERIMENTAL RESULTS AND DISCUSSION

The wideband spectra for three pumping scenarios are shown in Fig. 7: FW pumping, BW pumping, and bidirectional pumping. The power per pump was 29.73 dBm (940 mW), which was chosen from error-vector magnitude (EVM) optimisation of the 1651-nm signal. To demonstrate the importance of each pump for signal amplification, the amplified spectra of a CW signal at 1651 nm are shown in the figure. A comparison between the FW and BW pumping configurations shows that the former helps maintain a high OSNR, whilst the latter boosts the signal power at the output. Indeed, on their own, FW pumping leads to a low output power of -47 dBm at the end of the transmission line and BW pumping leads to a low OSNR. This is shown in the inset of Fig. 7, which shows the signal spectrum at the output in the BW pumping configuration. The inset also shows the output in the case of bidirectional pumping. It is clear that the benefit of this latter case in such a long span is that the signal power is maintained at a sufficiently high level for detection while its OSNR experiences a relatively small penalty.

Fig. 8 provides a distance-resolved plot of signal power and OSNR. It was measured by inserting a 99:1 coupler between each of the six NZDSF spools. In the signal power plots, the FW and BW pumping cases are associated with gain only at the beginning or the end of the transmission fibre, respectively (as expected), whilst the bidirectionally pumped configuration experiences gain at both ends. The output signal power can be seen to be almost the same in the FW and BW pumping cases, since the FW and BW pump powers are identical. As for the OSNR, the output OSNR in both the bidirectionally and FW pumping scenarios is 30.7 dB higher than that of the BW pumping scenario. The output OSNR of 33.9 dB and signal power of 0 dBm of the bidirectional pumping case suggest that an even longer reach transmission could be achieved.

To demonstrate the performance of the distributed RA in the transmission, three wavelengths (1641, 1646, and 1651 nm) were tested to determine the effect of total pump power on the

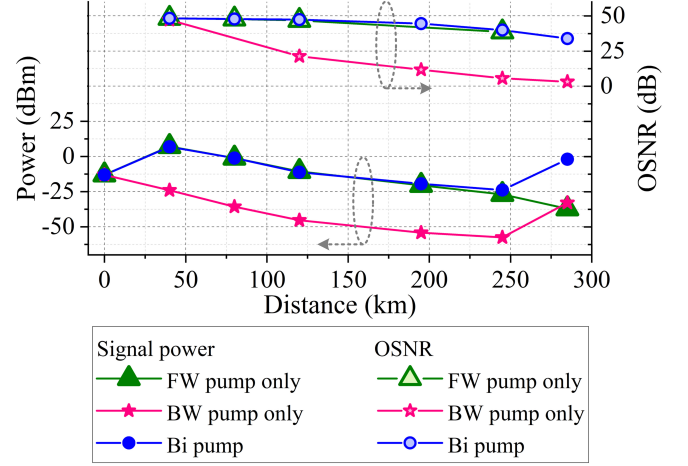


Fig. 8. Characterisations of the U-band distributed RA in terms of distance-resolved signal power and OSNR tested at 1651 nm.

quality of the received signal. These results are shown in Fig. 9(a). Note that each wavelength was transmitted individually, rather than in a WDM scenario, owing to the lack of multiple U-band sources for use in the setup. In this case, the pump powers were varied by changing the pump current of the EDFAs, whilst still maintaining $P_{FW} = P_{BW}$. The degradation in received EVM, termed *EVM penalty*, was measured by the ratio of the received EVM after transmission to the EVM of the signal before transmission. Using a total pump power higher than the optimum (1.88 W) may lead to signal degradation, likely due to Brillouin [23] and Kerr nonlinear effects.

The ratio between the FW and BW pump power, namely $R = 10 \log(P_{FW}/P_{BW})$, was varied next, whilst maintaining a fixed total pump power of $P_{FW} + P_{BW} = 1.88$ W. The effects of R on signal quality in terms of bit error ratio (BER) and EVM are presented in Fig. 9(b). The best values for both metrics were achieved when $R > 0$ dB, with the lowest EVM observed at $R = 0.25$ dB and the lowest BER at $R = 0.5$ dB. This performance enhancement beyond the 0-dB point is due to the improved OSNR resulting from FW pumping, whilst the difference between the optimal points of EVM and BER is because BPSK is relatively resilient to nonlinear distortions [24] (therefore, the BER can, at least for some time, decrease despite increasing phase noise and, hence, increasing EVM). Degradation beyond these values arises due to Kerr nonlinearity, as shown in the constellation diagrams in the inset of Fig. 9(b) as an increase in phase noise in the $R = 1$ dB case.

Fig. 9(c) provides spectra of the 1651-nm signal both back-to-back (B2B) and after transmission, with the relatively broad bandwidth of the filter visible from the residual ASE. Finally, the quality of the signals at the three tested wavelengths, as determined through BER measurements is shown in Fig. 9(d). A decrease in receiver sensitivity upon increasing the wavelength can be observed, which arose from the excess loss at longer wavelengths of devices which were not rated for use in the U-band. After transmission, no error floor can be detected, confirming that the amplification does not exhibit any deleterious levels of pump RIN transfer.

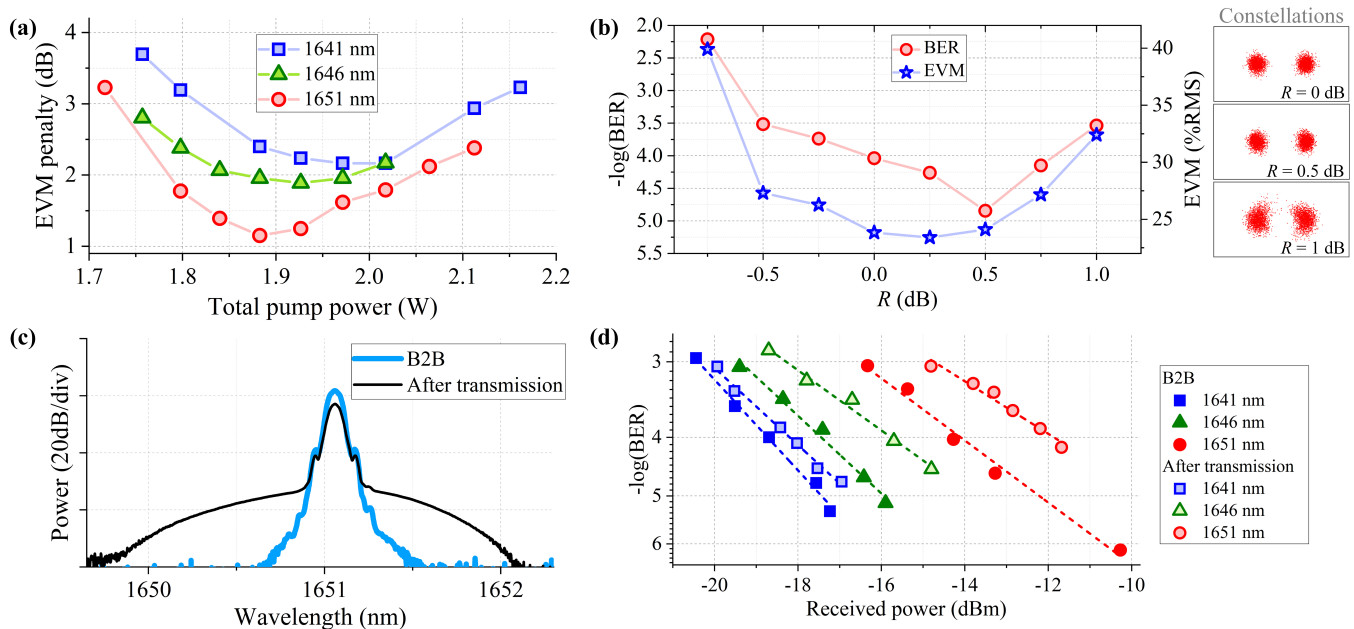


Fig. 9. Transmission results of (a) EVM penalty versus total pump power of the EDFAs at various wavelengths, (b) effect of pump power ratio on BER and EVM at 1651 nm (inset: x-pol constellations), (c) signal spectra of B2B and after transmission, and (d) BER versus received power at B2B and after transmission (the dashed lines indicate data's linear fit).

VI. CONCLUSION

We constructed and analysed a discrete RA to provide gain in the U-band by conveniently utilising a C-band EDFA as an ASE source to incoherently pump a 40-km long NZDSF. The experimental measurements confirm the benefits of using broadband incoherent pumping, which resulted in a flat, low NF of ~ 4 dB with a gain higher than 20 dB over a ~ 2.6 -THz bandwidth. We used the RA in a bidirectional pumping configuration to demonstrate ultra-long span transmission of a DP-BPSK signal over 285 km of NZDSF. This experiment is, at the time of writing, the longest single-span U-band transmission demonstrated. We believe that these results will encourage further investigation of the U-band for long-haul transmission and support research towards ultra-wideband, multi-band optical transmission.

VII. REFERENCES

- [1] R. Sadeghi, B. Correia, A. Souza, N. Costa, J. Pedro, A. Napoli, and V. Curri, "Transparent vs Translucent Multi-Band Optical Networking: Capacity and Energy Analyses," *Journal of Lightwave Technology*, vol. 40, no. 11, pp. 3486-3498, 2022.
- [2] P.J. Winzer, D.T. Neilson, and A.R. Chraplyvy, "Fiber-optic transmission and networking: the previous 20 and the next 20 years [Invited]," *Optics Express*, vol. 26, no. 18, pp. 24190-24239, 2018.
- [3] L. Rapp and M. Eiselt, "Optical Amplifiers for Multi-Band Optical Transmission Systems," *Journal of Lightwave Technology*, vol. 40, no. 6, pp. 1579-1589, 2022.
- [4] E. Pincemin, D. Grot, L. Bathany, S. Gosselin, M. Joindot, S. Bordaïs, Y. Jaouen, and J. Delavaux, "Raman gain efficiencies of modern terrestrial transmission fibers in S-, C- and L-band," in *Proc. Nonlinear Guided Waves and Their Applications (NLGW)*, Stresa, Italy, 2002, paper NLTuC2.
- [5] N.K. Thipparapu, Y. Wang, S. Wang, A.A. Umnikov, P. Barua, and J.K. Sahu, "Bi-doped fiber amplifiers and lasers [Invited]," *Optical Materials Express*, vol. 9, no. 6, pp. 2446-2465, 2019.
- [6] S.V. Firstov, S.V. Alyshev, K.E. Riumkin, V.F. Khopin, A.N. Guryanov, M.A. Melkumov, and E.M. Dianov, "A 23-dB bismuth-doped optical fiber amplifier for a 1700-nm band," *Scientific Reports*, vol. 6, no. 28939, pp. 1-6, 2016.
- [7] E.M. Dianov, "Bismuth-doped optical fibers: a challenging active medium for near-IR lasers and optical amplifiers," *Light: Science & Applications*, vol. 1, no. 15, p. 12, 2012.
- [8] C. Jiang, "Proposal of a Pr³⁺-doped telluride fiber amplifier for 1.3, 1.49, and 1.6 μ m transmission windows," *Applied Optics*, vol. 47, no. 36, pp. 6811-6815, 2008.
- [9] C. Jiang and P. Song, "6 - Broadband Fiber Amplifiers and Sources," in *Nonlinear-Emission Photonic Glass Fiber and Waveguide Devices*, Cambridge University Press, 2019, pp. 91-144.
- [10] S. Chen, Y. Jung, S. Alam, D.J. Richardson, R. Sidharthan, D. Ho, S. Yoo, and J.M.O. Daniel, "Ultra-short wavelength operation of thulium-doped fiber amplifiers and lasers," *Optics Express*, vol. 27, no. 25, pp. 36699-36707, 2019.
- [11] S.W. Harun, P. Poopalan, and H. Ahmad, "Gain enhancement in L-band EDFA through a double-pass technique," *IEEE Photonics Technology Letters*, vol. 14, no. 3, pp. 296-297, 2002.
- [12] J. Renaudier and A. Ghazisaeidi, "Scaling Capacity Growth of Fiber-Optic Transmission Systems Using 100+nm Ultra-Wideband Semiconductor Optical Amplifiers," *Journal of Lightwave Technology*, vol. 37, no. 8, pp. 1831-1838, 2019.
- [13] P.P. Baveja, D.N. Maywar, A.M. Kaplan, and G.P. Agrawal, "Self-Phase Modulation in Semiconductor Optical Amplifiers: Impact of Amplified Spontaneous Emission," *IEEE Journal of Quantum Electronics*, vol. 46, no. 9, pp. 1396-1403, 2010.
- [14] P.C. Reeves-Hall, D.A. Chestnut, C.J.S. De Matos, and J.R. Taylor, "Dual Wavelength Pumped L and U-Band Raman Amplifier," in *Optical Amplifiers and Their Applications*, Stresa, Italy, 2001.
- [15] M.A. Iqbal, M. Tan, and P. Harper, "RIN Transfer Mitigation Technique Using Broadband Incoherent Pump in Distributed Raman Amplified Transmission Systems," in *Proc. 2018 20th International Conference on Transparent Optical Networks (ICTON)*, Bucharest, Romania, 2018, paper Th.A4.3.
- [16] T. Zhang, X. Zhang, and G. Zhang, "Distributed Fiber Raman Amplifiers With Incoherent Pumping," *IEEE Photonics Technology Letters*, vol. 17, no. 6, pp. 1175-1177, 2005.

- [17] W.S. Pelouch, "Raman Amplification: An Enabling Technology for Long-Haul Coherent Transmission Systems," *Journal of Lightwave Technology*, vol. 34, no. 1, pp. 6-19, 2016.
- [18] N. Taengnoi, K.R.H. Bottrill, Y. Hong, L. Hanzo, and P. Petropoulos, "Broadband Incoherently Pumped Raman Amplification for Ultra-Long Span U-band Transmission Systems [Highly Scored]," in *Proc. 2022 European Conference on Optical Communications (ECOC)*, Basel, Switzerland, 2022, paper We4A.1.
- [19] S. Liang, S. Jain, L. Xu, K.R.H. Bottrill, N. Taengnoi, M. Guasoni, P. Zhang, M. Xiao, Q. Kang, Y. Jung, P. Petropoulos, and D.J. Richardson, "High Gain, Low Noise, Spectral-Gain-Controlled, Broadband Lumped Fiber Raman Amplifier," *Journal of Lightwave Technology*, vol. 39, no. 5, pp. 1458-1463, 2021.
- [20] C.R.S. Fludger, V. Handerek, and R.J. Mears, "Pump to signal RIN transfer in Raman fiber amplifiers," *Journal of Lightwave Technology*, vol. 19, no. 8, pp. 1140-1148, 2001.
- [21] D. Derickson, "Characterization of Erbium-Doped Fiber Amplifiers," in *Fiber optic test and measurement*, Englewood Cliffs, New Jersey, Prentice-Hall, 1998, pp. 519-595.
- [22] R. Hui, Y. Akasaka, and P. Palacharla, "Investigation of Forward and Backward Pumped Distributed Raman Amplification Schemes for a Single-Span 600Gb/s Coherent Fiber System," in *2021 Opto-Electronics and Communications Conference (OECC)*, Hong Kong, 2021.
- [23] A. Kobayakov, M. Mehendale, M. Vasilyev, S. Tsuda, and A.F. Evans, "Stimulated Brillouin scattering in Raman-pumped fibers: a theoretical approach," *Journal of Lightwave Technology*, vol. 20, no. 8, pp. 1635-1643, 2002.
- [24] C. Behrens, D. Lavery, D.S. Millar, S. Makovejs, B.C. Thomsen, R.I. Killey, S.J. Savory, and P. Bayvel, "Ultra-long-haul transmission of 7×42.9 Gbit/s PS-QPSK and PDM-BPSK," *Optics Express*, vol. 19, no. 26, pp. B581-B586, 2011.